



## OPEN A singular, broadly-applicable model for estimating on- and off-path walking travel rates using airborne lidar data

Michael J. Campbell<sup>✉</sup>, Sierra L. Cutler & Philip E. Dennison

Accurate prediction of walking travel rates is central to wide-ranging applications, including modeling historical travel networks, simulating evacuation from hazards, evaluating military ground troop movements, and assessing risk to wildland firefighters. Most of the existing functions for estimating travel rates have focused on slope as the sole landscape impediment, while some have gone a step further in applying a limited set of multiplicative factors to account for broadly defined surface types (e.g., “on-path” vs. “off-path”). In this study, we introduce the Simulating Travel Rates In Diverse Environments (STRIDE) model, which accurately predicts travel rates using a suite of airborne lidar-derived metrics (slope, vegetation density, and surface roughness) that encompass a continuous spectrum of landscape structure. STRIDE enables the accurate prediction of both on- and off-path travel rates using a single function that can be applied across wide-ranging environmental settings. The model explained more than 80% of the variance in the mean travel rates from three separate field experiments, with an average predictive error less than 16%. We demonstrate the use of STRIDE to map least-cost paths, highlighting its propensity for selecting logically consistent routes and producing more accurate yet considerably greater total travel time estimates than a slope-only model.

**Keywords** Walking speed, Pedestrian travel rates, Airborne lidar, Human–environment interaction, Least-cost path modeling

From mapping historical transportation networks using least-cost path modeling to estimating the amount of time needed for a wildland firefighter to evacuate to safety, accurate prediction of walking travel rates is pivotal in a diverse array of applications and scientific disciplines<sup>1,2</sup>. Although a number of existing travel rate functions exist, they fail to sufficiently account for the vast diversity of landscape conditions that impede foot travel<sup>3–11</sup>. In this study, we introduce a broadly applicable mathematical function for predicting and mapping travel rates that leverages airborne lidar’s impressive capacity for quantifying three-dimensional vegetation and terrain structure at a high spatial resolution. Trained and validated on field experiments conducted across a variety of environments and bolstered by a comparison to crowdsourced data, the Simulating Travel Rates In Diverse Environments (STRIDE) model provides a new, generalizable framework for predicting travel times and mapping travel routes in both developed and wildland settings.

The influence of slope on travel rates has been investigated as early as the late nineteenth century<sup>4</sup>. Massive growth in the use of global navigation satellite system-enabled smart devices, the advancement of geospatial modeling techniques, and increasingly precise terrain models from sources such as airborne lidar have all contributed to improved ability to predict travel rates as a function of terrain slope<sup>7,12–14</sup>. Starting with Tobler<sup>3</sup>, the development of pedestrian travel rate functions has fostered a wide variety of applications in disciplines such as archaeology, emergency response and safety, health care access, recreation management, and urban planning<sup>15–19</sup>.

Although it plays a critical role in dictating pedestrian movement, slope is only one of multiple landscape characteristics that may impact travel rates. The presence, abundance, structure, and distribution of vegetation also have major limiting effects on the ease with which one can move through a landscape<sup>20–22</sup>. Shorter vegetation at or near the ground surface (i.e., grasses, forbs, shrubs) can affect foot placement and alter gait. Taller shrubs and trees can impact movement in a variety of ways, ranging from avoidance (i.e., moving around obstacles deemed impossible) to impedance (i.e., moving through possible vegetation but being physically restrained by

School of Environment, Society and Sustainability, University of Utah, 260 South Central Campus Drive, Salt Lake City, UT 84112, USA. <sup>✉</sup>email: mickey.campbell@ess.utah.edu

it). Likewise, the roughness of the ground surface itself can act as an additional impediment to travel<sup>12</sup>. Walking on or around a boulder field requires more time than walking on a paved surface, for example.

Based on past research, walking travel rates and times can be reliably predicted in situations in which slope is the dominant factor and variability in vegetation density and surface roughness is minimal. These conditions are met in urban and other developed settings, where movement is expected to take place on roads or other well-maintained, hard surfaces<sup>23–25</sup>, and for “on-path” travel, where surface roughness is assumed to be uniform and vegetation density is negligible<sup>3,5,10</sup>. However, there are many applications (e.g., military, search and rescue, wildland firefighting) for which it is essential to also predict travel behaviors in off-road, off-trail (henceforth collectively referred to as “off-path”) settings. Past work has accommodated off-path environments by lumping the vast diversity of landscape characteristics into a single multiplier<sup>3,6</sup> or a small number of fixed multipliers specific to broad land cover categories<sup>7,22</sup>. There remains a need to develop a singular travel rate predictive equation that can encompass both on- and off-path travel and that provides for continuous estimation of off-path travel rates.

With the overarching goal of increasing the accuracy and broad applicability of walking travel rate and time predictions for both on-path and off-path travel, we developed the STRIDE model. STRIDE is based on continuous variables derived from airborne lidar data that represent terrain slope, vegetation density, and surface roughness (Fig. 1). Discrete-return airborne lidar is unique in its ability to map three-dimensional structure over space based on point clouds representing the x, y, and z coordinates of reflective surfaces (e.g., ground and vegetation). Narrow laser pulses exploit small gaps in vegetation canopies to measure ground elevations with high precision, and even in the presence of tall vegetation, airborne lidar can characterize the structure of vegetation within the aboveground height ranges that are most relevant to human movement<sup>26–29</sup>. In this paper, we describe model performance against travel rates gleaned from three field experiments, the sensitivity of the model to landscape parameters derived from airborne lidar data, and compare STRIDE to a recent set of travel rate models derived from a large, crowdsourced database of GPS tracks representing on-path travel. Additionally, we demonstrate the application of the model in the context of least-cost path simulation, highlighting the importance of evaluating landscape conditions beyond just terrain slope for estimating travel times.

## Results and discussion

### Vegetation density and surface roughness geometry

The STRIDE model best explained travel rates using a surface roughness focal radius of 2 m and a vegetation density height range of 0.85–1.20 m (Fig. 2), producing a cross-validated  $R^2$  of 0.806 and an RMSE of  $0.168 \text{ ms}^{-1}$  (16% of the mean travel rate measured in our experiments). For an individual with an average height of 1.70 m, this vegetation height range approximately represents waist-to-chest height. The vegetation in this range was too high to step or climb over and too low to duck under when walking along vegetated transects. Although the 0.85–1.20 m range was found to perform best in our study area, there was a cluster of comparable height ranges from 0.45 to 1.70 m (approximately knee to top of head for an average height person) whose predictive error was less than 2% greater than that of the best model (Supplementary Table S1). Using a larger height range could

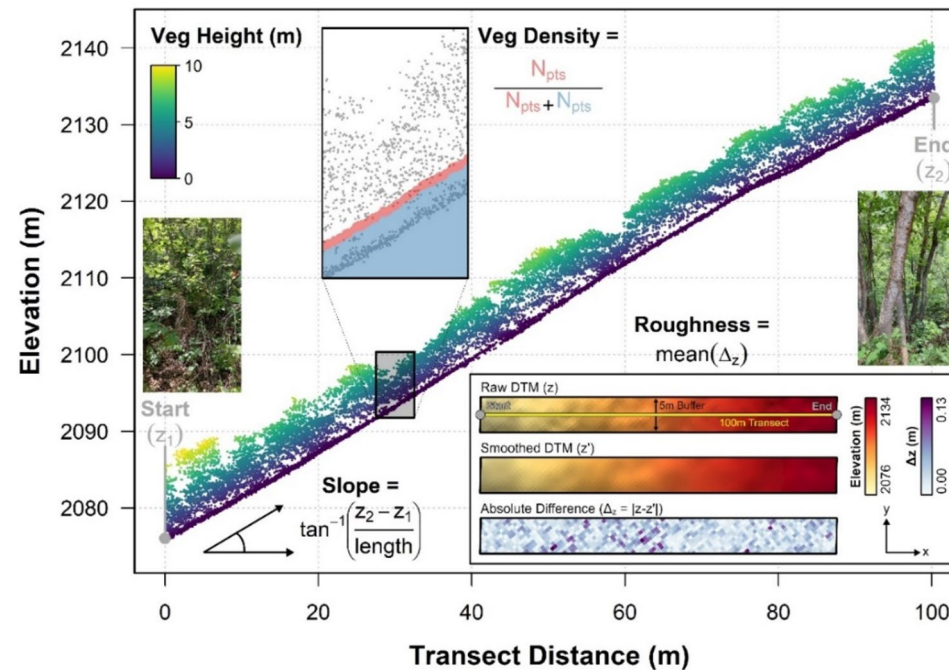


**Fig. 1.** The lidar-derived landscape conditions considered in the STRIDE model. Landscape slope, surface roughness, and vegetation density captured by airborne lidar data for one experimental transect used in this study.

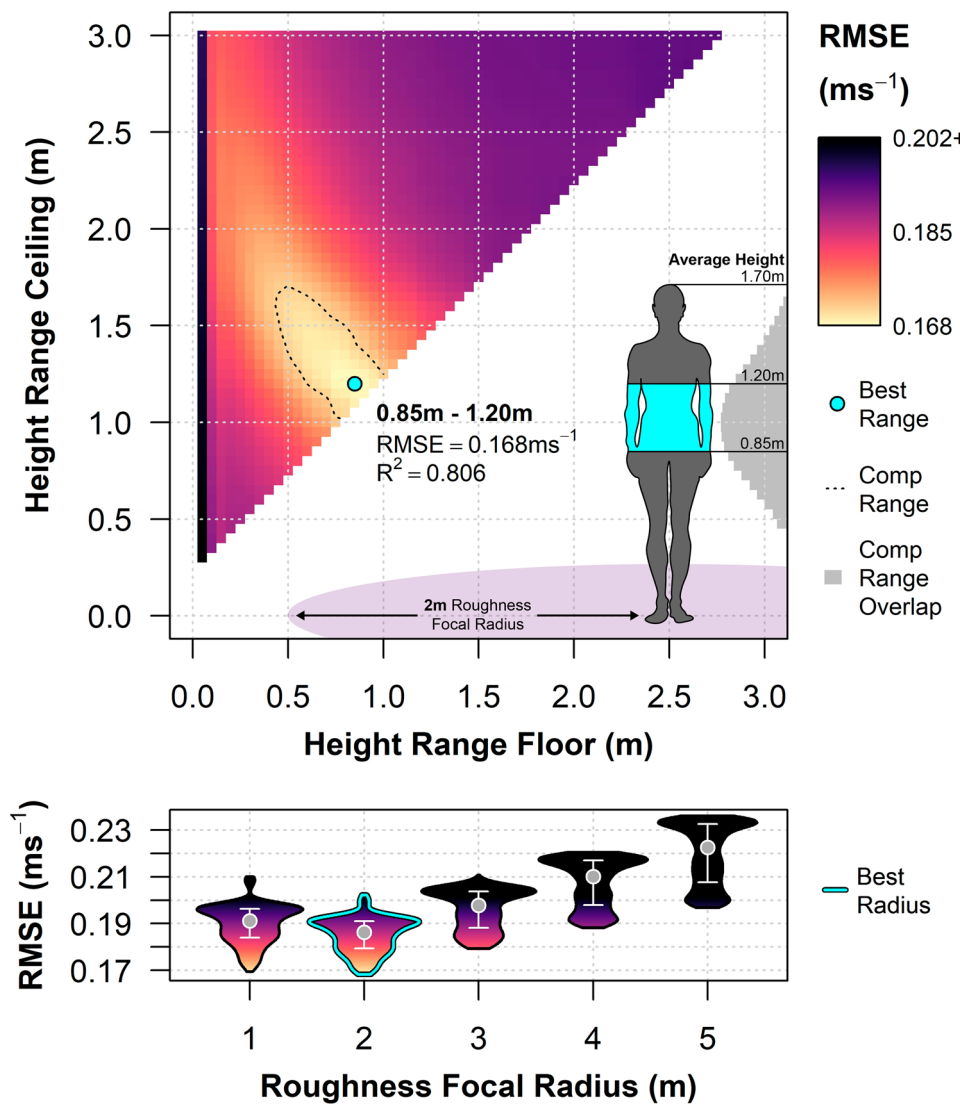


**Fig. 2.** The spatial dimensions of vegetation density and ground surface roughness effects on travel rates. Plots showing cross-validated model prediction errors for different surface roughness focal radii (bottom) and vegetation density height ranges (top). The radius and height range with the best model performance are highlighted and depicted in the context of a human with an average height of 1.70 m. The comparable (“comp”) ranges, within which the model RMSEs were within 2% of the best model, are also highlighted to illustrate a broader array of height floors and ceilings that can be used for estimating travel rates in STRIDE with similar predictive performance. The comp range overlap histogram illustrates the relative number of times each 0.05 m wide vertical range was represented in the comp ranges.

provide advantages where the near-surface lidar point density is relatively sparse by increasing the number of points sampled within the range.

#### STRIDE model performance

A cross-validated comparison between the observed and STRIDE-predicted travel rates revealed a highly linear correlation (Fig. 3). The relationships between travel rates and the three landscape metrics of interest are clear, with steeper slopes, denser vegetation, and rougher ground surfaces contributing to lower travel rates. A final model built using all the data (rather than withholding one transect for cross-validation) yielded a residual standard error of  $0.159 \text{ ms}^{-1}$ . This residual error and the ~19% of variance left unexplained in the cross-validation may be attributable to variety of factors, including different fitness levels in the three groups of study participants<sup>30</sup>, different weather conditions experienced during the three experiments (i.e., August vs. September vs. January)<sup>31</sup>, and different altitudes of the study transects<sup>32</sup>.

The final STRIDE model was defined according to Eq. (1), where the coefficients  $a$ ,  $b$ ,  $c$ ,  $d$ , and  $e$  are found in Table 1.

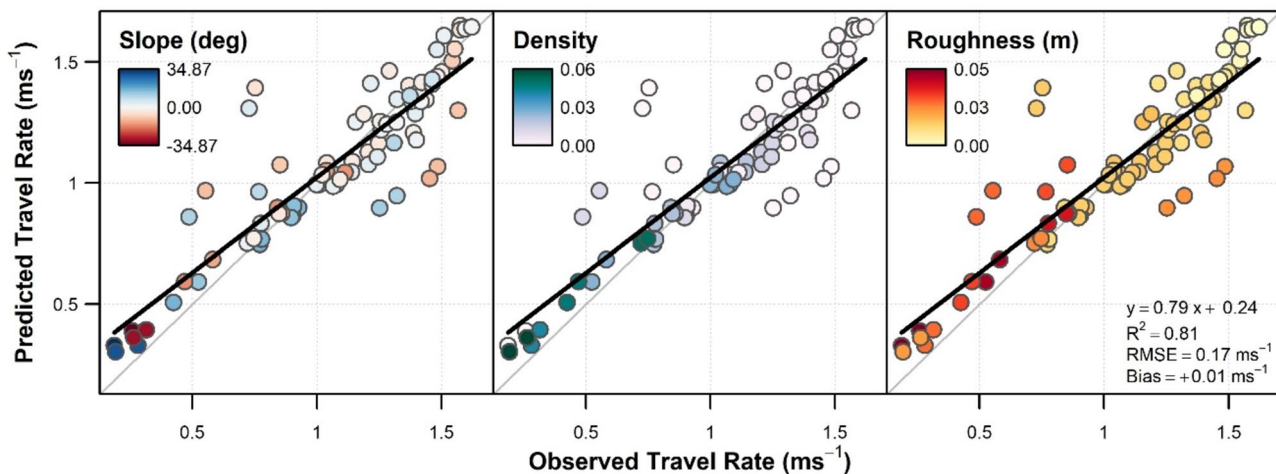


**Fig. 3.** Performance of the travel rate predictive model. Predicted versus observed travel rates for STRIDE based on leave-one-transect-out cross-validation. Plots are identical except for the coloring representing each predictor variable. The thin gray line represents the 1:1 relationship between the predictions and observations, and the thick black line represents the linear trend between them, the statistics for which can be found at the bottom right.

Coefficient	Estimate	SE	t	p	Significance
a	-2.320	0.981	-2.365	0.021	*
b	26.315	2.515	10.462	< 0.001	***
c	147.362	16.302	9.040	< 0.001	***
d	15.265	2.916	5.235	< 0.001	***
e	16.505	3.837	4.302	< 0.001	***

**Table 1.** STRIDE coefficients. Nonlinear least squares (NLS) regression results for the STRIDE model based on vegetation density within the 0.85–1.20 m height range using all transects, using coefficients shown in Eq. (1). The levels of significance are denoted as \*\*\*, \*\*, and \*, at alpha levels of 0.001, 0.01, and 0.05, respectively. Supplementary Table S1 provides the coefficients for all height ranges with cross-validated errors of 2% of the best height range.

$$travelrate = \frac{c \left( \frac{1}{\pi b \left( 1 + \left( \frac{slope - a}{b} \right)^2 \right)} \right)}{1 + d \times density + e \times roughness} \quad (1)$$

The numerator represents the relationship between slope and travel rate and is based on the Lorentzian function, and the denominator acts to reduce travel rates in the presence of vegetation or rough ground surfaces.

### Broad applicability of STRIDE

STRIDE demonstrated an impressive ability to predict on- and off-path walking travel rates, especially when considering the diversity of the data used to construct it. We used data from three different experiments conducted at different times in different study areas with landscape conditions mapped using four different lidar datasets and with travel rates derived from different pools of study subjects. Despite the diversity of inputs, a single predictive model was able to account for more than 80% of the variance in group mean travel rates. The fact that the model capably integrated travel rates from both off-path and on-path conditions is particularly noteworthy. Furthermore, comparing the range of landscape conditions tested in our experiments to a random sample of natural landscapes in the U.S. revealed that our transects captured the 99th percentile of the sample slope, 92nd percentile of the sample vegetation density, and 73rd percentile of the sample surface roughness (Fig. 4). Thus, the STRIDE model should be broadly applicable, with little need for extrapolation.

A STRIDE model using no vegetation cover and median trail surface roughness was nearly identical to the 67.5th percentile travel rate function from a study of a large, diverse, crowdsourced dataset representing on-path travel<sup>5</sup> (RMSE = 0.018 ms<sup>-2</sup>; bias = +0.005 ms<sup>-2</sup>; R<sup>2</sup> = 0.996). These results suggest that STRIDE can accurately capture the on-path relationships between slope and travel rate, with the caveat that the subjects walking 100 m transects moved slightly faster than the average hiker in the crowdsourced dataset. We attribute this to the fact that 100 m transects do not induce large fatigue effects, while longer hikes produce slightly slower travel rates

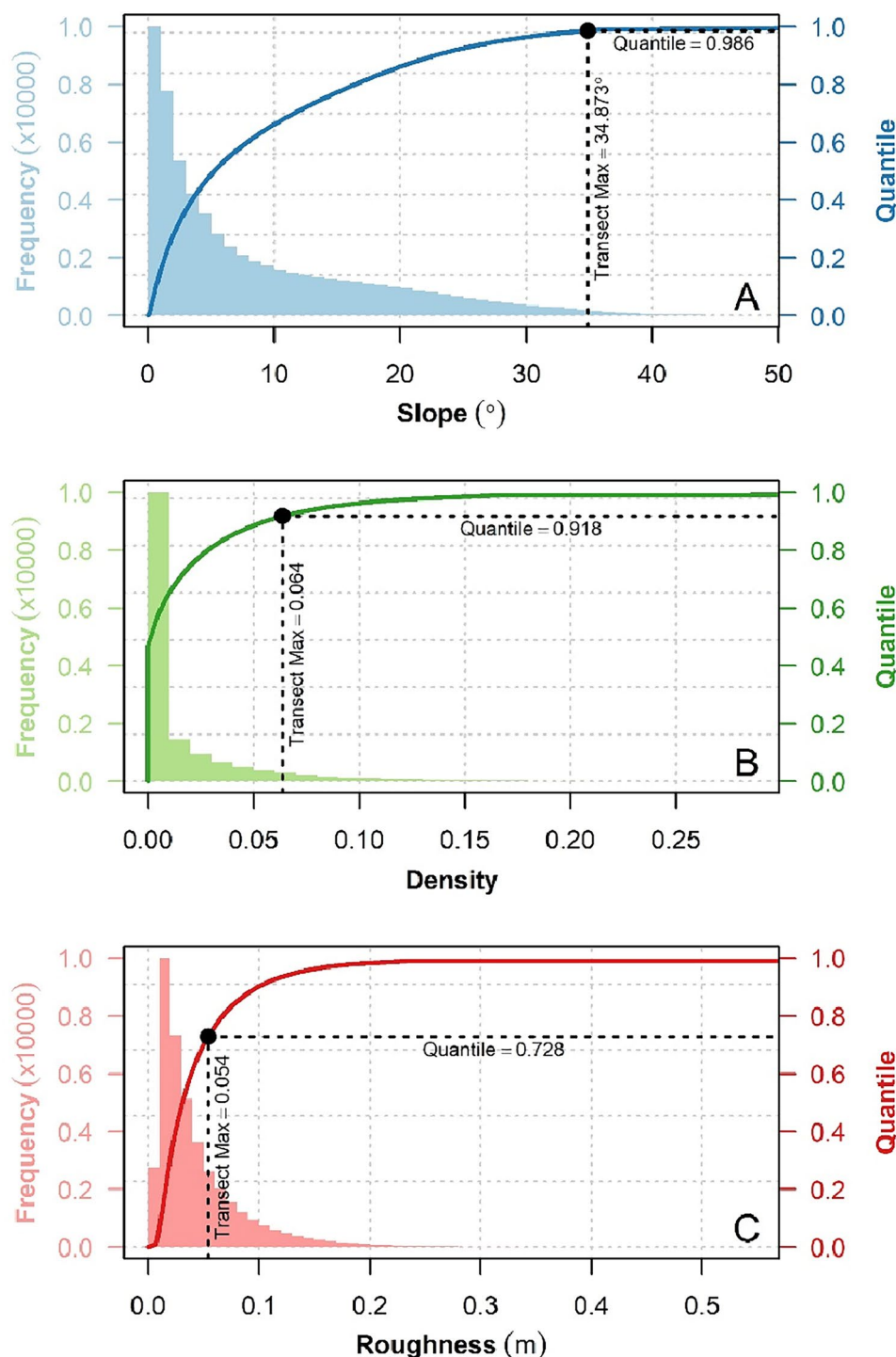


**Fig. 4.** Representativeness of our experimental transects. Comparison between the slope (A), vegetation density (B), and ground surface roughness (C) of our experimental transects and distributions of the same variables from 1 M random points placed within 100 random natural areas of the contiguous US. The colored histograms represent the 1 M point distributions of each landscape variable. Darker-colored solid lines represent the quantiles of those distributions. The black points and associated dashed lines represent the highest value of each landscape metric within the experimental transects and the approximate quantile within the 1 M point sample. In all three figures, the range of values shown is limited to the 0–99.9th quantile for clarity.

due to fatigue. However, we expect that the relative effects of landscape conditions on travel rates should be scalable—that is, steeper slopes, denser vegetation, and rougher ground surfaces should impede pedestrian travel similarly on short (e.g., 100 m) and longer-distance (e.g., 1 km +) walks. Accordingly, we suggest that STRIDE could be used to generate longer-distance least-cost paths; however, to use these paths for travel time estimation would require that a scaling factor be added.

One limitation to broad applicability of STRIDE is the lack of globally available airborne lidar data. In the US, thanks to the USGS 3D Elevation Program<sup>33</sup>, there is widespread, freely available lidar data; however, in many other parts of the globe these data are much more limited. There are several sources of global or near-global digital elevation models that could be used for slope mapping, but ground surface roughness and vegetation density require lidar. In the absence of lidar data, there may be ways to approximate these variables. For example, using a sample of lidar and some widely available predictor data, one might be able to model ground surface roughness and vegetation density using some knowledge of land cover or vegetation type, topography, soil type, and bedrock geology. Future work should aim to better understand the extent to which these valuable predictors of human movement can be modeled in the absence of lidar data, and the degree to which such modeled products would affect travel rate predictive accuracy.

### Applying STRIDE to least-cost path modeling

The routes generated from least-cost path models aimed at optimizing for slope-only—by far the most common approach for such models—and the STRIDE model combining slope, vegetation density, and surface roughness differed substantially (Fig. 5). The former tended to produce direct routes that ignore local landscape characteristics, whereas the latter generated more sinuous routes that appear to more consistently favor roadways, trails, and meadows with lower vegetation density and surface roughness. Even without the explicit addition of a transportation dataset, the STRIDE model clearly favored preexisting, easy-to-traverse paths, even when applied to a geographically complex urban environment (Supplementary Fig. S1). This represents an important advantage of STRIDE over a purely slope-based approach. STRIDE better approximates how pedestrians might identify their own optimal path on the ground in the absence of geospatial support, with a preference toward utilizing roads and trails to optimize travel between points on the landscape.

On average, the STRIDE-based travel times were 1.5 times greater than those computed from a slope-travel rate predictive model, highlighting the importance of incorporating a more holistic accounting of landscape impediments into off-path travel time estimation. Furthermore, our travel time estimates reveal an important degree of variability that would be left unaccounted for if fixed multiplicative terms were used to universally estimate off-path, slope-based travel times<sup>3,6,7</sup>. The importance of route selection and travel time estimate differences becomes particularly acute when placed in an applied context. For example, if the starting point in Fig. 5 represents a search and rescue team and the destination points represent injured hikers, taking a suboptimal route to reach a hiker or underestimating the time to arrival can both have dangerous consequences.

### STRIDE R package

To enable easy application of STRIDE, we developed an open-source *R* package called *stride* (<https://github.com/mickeycampbell/stride>). The package provides all of the functions needed to generate a least-cost path and estimate the travel time along that path, given an input airborne lidar point cloud dataset. The package's primary functions are briefly described as follows in the order that they are executed:

- *gen\_dtm()* interpolates a digital terrain model from airborne lidar, needed for estimating slope and ground surface roughness.
- *gen\_rgh()* generates a ground surface roughness raster dataset.
- *norm\_hgt()* normalizes lidar point heights relative to ground surface, needed for calculating vegetation density.
- *gen\_dns()* generates a vegetation density raster dataset.
- *get\_bars()* generates barrier raster datasets, representing impassable landscape features such as slopes greater than 45° and waterbodies.
- *align\_rasts()* ensures spatial congruency between cost and barrier rasters, necessary for building a transition matrix.
- *bld\_tm()* builds a transition matrix that quantifies movement cost between adjacent cells in the cost and barrier rasters.
- *map\_lcp()* maps the least-cost path between two or more supplied point locations and estimates the travel time along the path.

### Summary and Implications

STRIDE is a singular model that can predict walking travel rates and times along a full spectrum of landscape development, from urban to wild. In developed environments, travel rates and times are primarily dictated by the slope of paved paths. In wildland environments, slope, ground surface roughness, and vegetation density all contribute to travel impedance. In between those extremes, such as on hiking trails, slope and ground surface roughness will act as the primary factors reducing travel rates. With more than 80% of the variance in group-level mean travel rates accounted for across three different study areas and 16% travel rate predictive error, STRIDE demonstrated an impressive ability to predict travel rates across a wide range of slopes, surface roughness values, and vegetation densities. Future refinement of the STRIDE model may be possible by considering fatigue over longer distances and load carriage, adding experimental data for additional vegetation types and surface hazards, and quantifying the effects of surface moisture. As is, STRIDE should have broad applicability for estimating

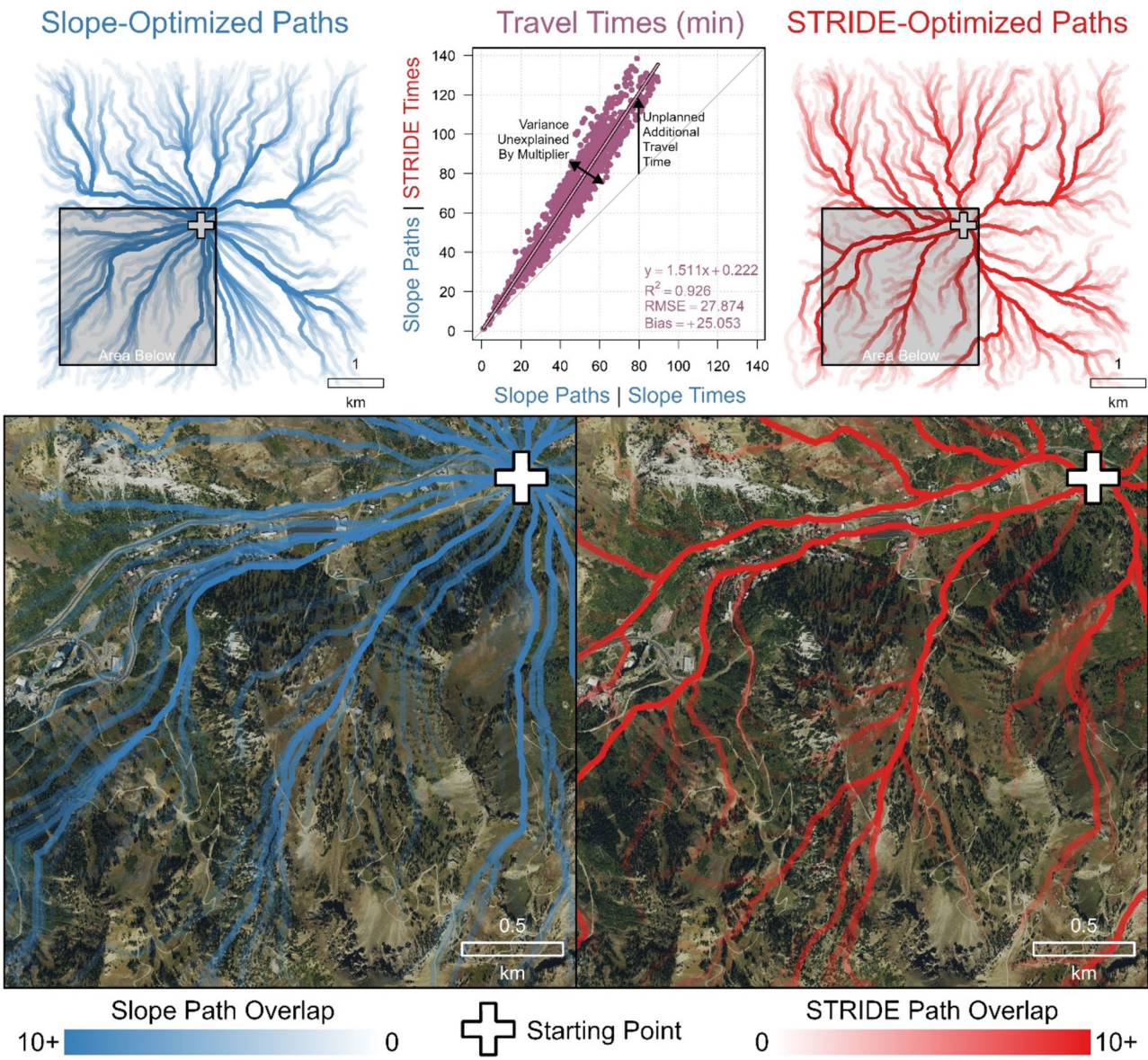


**Fig. 5.** Demonstration of STRIDE in least-cost path modeling. Least-cost paths connecting a central origin point with 1000 random destination points using two different travel rate models: one optimized only for terrain slope (blue paths, left) and the STRIDE model, which is optimized for slope, vegetation density, and surface roughness (red paths, right). In both cases, paths are drawn with 10% opacity, such that 10 + paths yield a fully opaque line on the maps. The scatterplot compares travel time estimates on slope-optimized least-cost paths calculated in two ways, based solely on slope-driven travel rates (x-axis) and based on STRIDE (y-axis). Background imagery is courtesy of the USDA National Agricultural Inventory Program.

walking travel rates used for modeling least-cost path travel across a wide range of disciplines, offering essential improvements over previous models. Future research may further refine STRIDE through instantaneous GPS tracking of pedestrians in a similar experimental context to understand finer-scale patterns of speed and route selection than our transect-level analysis could reveal.

## Methods

### Travel rate experiments

In this study, we used travel rate data from three field experiments in which subjects walked transects approximately 100 m in length through varied landscapes with existing airborne lidar data. In all three experiments, the subjects were timed as they walked each transect twice, once in each direction, facilitating the analysis of both upslope and downslope travel rates. The mean travel rate among all study subjects was computed for each direction of each transect, which served as the dependent variable of the STRIDE model. The transects in each experiment were optimized to capture the diversity of landscape conditions within each study site while also possessing relative uniformity in slope, vegetation type, and vegetation density along each transect. We sought within-transect uniformity because our study design was focused on transect-level mean travel rates.

The first experiment took place in September 2016, when up to 31 study subjects walked 22 transects through varying vegetation densities within a juniper-sagebrush woodland near Levan, Utah, USA<sup>21</sup> (Supplementary Fig. S2). A bootstrapping analysis of travel rates revealed that transect mean travel rates could be approximated to within  $\pm 5\%$  using just five subjects. We reduced the number of subjects in the subsequent experiment to minimize alteration of vegetation and surface characteristics caused by repeated travel. The second experiment took place in August 2023 in and around the central Wasatch Mountains in Utah with the intent of capturing a wider and more broadly representative set of undeveloped, off-path landscape conditions than did the first experiment (Supplementary Fig. S3). Up to nine study subjects walked 11 transects through highly varied landscapes, ranging from sparsely vegetated flat areas to very steep forested areas. The vegetation types included grass/herbaceous meadow, sagebrush shrubland, and multiple types of broadleaf deciduous forest and mixed conifer forest with varying understory vegetation densities. To capture low-roughness, on-path travel, we conducted a third travel rate experiment within an urban area of Salt Lake City, Utah (Supplementary Fig. S4). We identified eight paved transects with no vegetation that spanned a range of slopes, along which eight study subjects walked in January 2024. University of Utah's Institutional Review Board approved all the study protocols prior to engaging in the experiments, which were performed in accordance with the Board's guidelines and regulations, including the prior obtainment of informed consent by all study participants.

### Lidar-Derived landscape impediments

The three independent variables used to predict travel rates, all derived from lidar data, were slope, vegetation density, and surface roughness (Fig. 1). The transect-level travel rates, slopes, densities, and roughness values for all transects can be found in Supplementary Fig. S5. Four different lidar datasets were needed to cover all of the transects in Study Areas 1, 2, and 3 (Supplementary Table S2). All lidar data were acquired from the USGS 3D Elevation Program<sup>33</sup>. Points were first filtered to remove those classified by the vendor as noise, including point classes 7 and 18 according to the LAS 1.4 specification<sup>34</sup>, which represent faulty lidar point returns far above or below reasonable elevation values. There are many noise classification algorithms, and we do not know which among them were used for the lidar data we acquired from the USGS for this study, but removal of noise is considered standard practice in lidar data analysis for improving the data<sup>35</sup>. The resulting cleaned point clouds were used to derive high-resolution (1 m) digital terrain models (DTMs) through triangulated irregular network-based interpolation of classified ground points. For the purpose of quantifying vegetation structure, raw elevations were converted to aboveground heights for all nonground points by subtracting point elevations from the DTM. All lidar data processing was performed in *R* using the *lidR* library<sup>36,37</sup>. The transect slope was calculated in degrees based on the x, y, and z coordinates of the transect start and end points. The surface roughness captures meter-scale undulations in the substrate (e.g., soil, rocks, litter) as well as ground-level vegetation and was based on the 1 m resolution DTM. The DTM was cropped to a 5 m buffer around each transect. Within each cropped DTM, roughness (in meters) was equal to the average absolute difference between the raw terrain elevations and smoothed elevations resulting from a focal mean using a circular neighborhood with a fixed radius<sup>38</sup>. We tested five different focal radii to determine what roughness scale would be most predictive of travel rates: 1 m, 2 m, 3 m, 4 m, and 5 m.

The normalized relative density (NRD) of lidar point returns was used as a proxy for vegetation density<sup>26</sup>. To calculate the NRD, the same 5 m-buffered transect boxes were used to clip a spatially coincident subset of ground height-normalized lidar points. The NRD is the number of lidar points within a particular height range divided by the number of lidar points less than the ceiling of that height range, representing the proportion of lidar pulse energy intercepted by low-lying vegetation prior to reaching the ground surface. We tested a variety of height ranges to determine which would be most directly linked to travel impedance: every height range floor-ceiling combination from 0.05 to 3.00 m at a 0.05 m interval, such that the ceiling was always at least 0.25 m higher than the floor (e.g., 0.05–0.30 m, 0.05–0.35 m, [...], 2.70–3.00 m, 2.75–3.00 m). In all, this yielded 1540 unique height ranges, each of which served as a test range for computing vegetation density.

### Model development and performance assessment

To construct the STRIDE model, we modeled travel rates as a function of slope, roughness, and vegetation density. We used nonlinear least squares regression modeling, which requires the provision of a function form to which to fit coefficients. Based on our previous work<sup>5,8,39</sup> and preliminary testing, we identified the function form of Eq. (1) as a suitable basis for modeling. To assess model performance, we used a leave-one-transect-out cross-validation approach and relied on the coefficient of determination ( $R^2$ ), root mean squared error (RMSE), and bias between observed and predicted travel rates as performance evaluation metrics.

### Assessing the broad applicability of STRIDE

To examine the degree to which the experimental transects captured a broadly representative range of landscape conditions, we compared transect-derived estimates of slope, vegetation density, and surface roughness to those from a random sample of landscapes in the U.S. One hundred random points were placed within the contiguous US in undeveloped and uncultivated land areas (as mapped by the 2021 National Land Cover Database<sup>40</sup>) with recent (2018–2024) USGS 3D Elevation Program airborne lidar of at least quality level 2 (nominal pulse density of at least two pulses per square meter). Within the singular lidar tiles intersecting each point, the slope, density, and roughness were mapped at 10 m resolution, and 10,000 random pixel values were extracted (1 M points in total). Our steepest, densest, and roughest transects were compared to the 1 M-point sample to determine the approximate quantile they represented.

To compare the STRIDE model to an independent set of on-path models derived from crowdsourced GPS hiking data from AllTrails, we calculated the linear roughness of 20 hiking trails, as described in Campbell et al.<sup>5</sup>.

Points were placed every 1 m along each trail, and 1 m lidar-derived terrain elevations were extracted at each point. The average difference between the raw elevations and the rolling mean elevations within a 5-point (i.e., 2 m-radius) moving window was used to represent trail-wide roughness. The average among all 20 trails, found to be 0.03 m, was used as the roughness value in STRIDE, along with 0% vegetation density, to make travel rate predictions for a range of slopes ( $-45^\circ$  to  $45^\circ$ ). The resulting predictions were compared to those of each of the 39 percentile models (2.5th–97.5th percentiles at an interval of 2.5) from Campbell et al.<sup>5</sup> to assess the similarity between experimentally derived and crowdsourced predictions based on nearly 2000 hikes (Supplementary Fig. S6).

### Applying STRIDE to least-cost path modeling

To demonstrate the utility of STRIDE, we provide an example application focused on least-cost path modeling. Least-cost path modeling is among the most common applications of travel rate functions<sup>41,42</sup>, enabling the identification of routes that minimize travel time between two (or more) points on a landscape. Using a mountainous, mixed-use  $6 \times 6$  km area surrounding Alta, Utah, as a case study, least-cost paths were generated from a central origin point to 1000 random destination points. Two different types of paths were generated: (1) one that used only the terrain slope as the sole landscape impediment and (2) one that used the slope, vegetation density, and ground surface roughness as impediments. In the former case, we used Campbell et al.'s<sup>5</sup> crowdsourced 50th percentile slope-travel rate function to identify the least-cost paths; in the latter case, we used STRIDE. In both cases, slopes greater than 45 degrees, National Hydrography Dataset-mapped water bodies<sup>43</sup>, and Microsoft Building Footprint-mapped buildings<sup>44</sup> were treated as impassable landscape barriers. In addition to comparing the spatial dimensions of the resulting least cost paths, we also compared estimated travel times on the slope-optimized paths predicted using the slope-based travel rate function and STRIDE to gain insight into how underestimated travel times are when vegetation and surface roughness are ignored. To test the performance of STRIDE in an urban setting, we generated least-cost paths between 1000 random start–end point pairs in a  $4 \times 4$  km area of Salt Lake City, UT, comparing the spatial dimensions of path overlap to the transportation network to assess the degree to which paths followed roads. All least-cost path modeling was performed in R with reliance on the *terra*, *raster*, and *gdistance* packages<sup>36,45–47</sup>.

### Data availability

The datasets generated during and/or analyzed during the current study are available from the corresponding author on reasonable request.

Received: 25 March 2024; Accepted: 27 August 2024

Published online: 13 September 2024

### References

1. Fryer, G. K., Dennison, P. E. & Cova, T. J. Wildland firefighter entrapment avoidance: Modelling evacuation triggers. *Int. J. Wildland Fire* **22**, 883–893 (2013).
2. Kealy, S., Louys, J. & O'Connor, S. Least-cost pathway models indicate northern human dispersal from Sunda to Sahul. *J. Hum. Evol.* **125**, 59–70 (2018).
3. Tobler, W. *Three Presentations on Geographical Analysis and Modeling*. 24 (1993).
4. Naismith, W., Cruach Adran, Stobinian, and Ben More. *Scottish Mountain Club J.* **2**, 136 (1892).
5. Campbell, M. J., Dennison, P. E. & Thompson, M. P. Predicting the variability in pedestrian travel rates and times using crowdsourced GPS data. *Comput. Environ. Urban Syst.* **97**, 101866 (2022).
6. Irmischer, I. J. & Clarke, K. C. Measuring and modeling the speed of human navigation. *Cartogr. Geogr. Inf. Sci.* **45**, 177–186 (2018).
7. Wood, A., Mackaness, W., Simpson, T. I. & Armstrong, J. D. Improved prediction of hiking speeds using a data driven approach. *PLOS ONE* **18**, e0295848 (2023).
8. Sullivan, P. R., Campbell, M. J., Dennison, P. E., Brewer, S. C. & Butler, B. W. Modeling wildland firefighter travel rates by terrain slope: Results from GPS-tracking of type 1 crew movement. *Fire* **3**, 52 (2020).
9. Prisner, E. & Sui, P. Hiking-time formulas: A review. *Cartogr. Geogr. Inf. Sci.* **50**, 421–432 (2023).
10. Rees, W. G. Least-cost paths in mountainous terrain. *Comput. Geosci.* **30**, 203–209 (2004).
11. Pandolf, K. B., Givoni, B. & Goldman, R. F. Predicting energy expenditure with loads while standing or walking very slowly. *J. Appl. Physiol. Respir. Environ. Exerc. Physiol.* **43**, 577–581 (1977).
12. Rout, A., Nitolslawski, S., Ladle, A. & Galpern, P. Using smartphone-GPS data to understand pedestrian-scale behavior in urban settings: A review of themes and approaches. *Comput. Environ. Urban Syst.* **90**, 101705 (2021).
13. Zangenehnejad, F. & Gao, Y. GNSS smartphones positioning: Advances, challenges, opportunities, and future perspectives. *Satell. Navig.* **2**, 24 (2021).
14. Hodgson, M. E. & Bresnahan, P. Accuracy of airborne lidar-derived elevation. *Photogram. Eng. Remote Sens.* **70**, 331–339 (2004).
15. Bird, M. I., O'Grady, D. & Ulm, S. Humans, water, and the colonization of Australia. *Proc. Natl. Acad. Sci.* **113**, 11477–11482 (2016).
16. Wood, N. J., Jones, J., Spielman, S. & Schmidlein, M. C. Community clusters of tsunami vulnerability in the US Pacific Northwest. *Proc. Natl. Acad. Sci.* **112**, 5354–5359 (2015).
17. Weiss, D. J. et al. A global map of travel time to cities to assess inequalities in accessibility in 2015. *Nature* **553**, 333–336 (2018).
18. Márquez-Pérez, J., Vallejo-Villalta, I. & Álvarez-Francoso, J. I. Estimated travel time for walking trails in natural areas. *Geografisk Tidsskrift-Danish J. Geogr.* **117**, 53–62 (2017).
19. Dacey, K., Whitsed, R. & Gonzalez, P. Using an agent-based model to identify high probability search areas for search and rescue. *Aust. J. Emerg. Manag.* **37**, 88–94 (2022).
20. Anguelova, Z., Stow, D. A., Kaiser, J., Dennison, P. E. & Cova, T. Integrating fire behavior and pedestrian mobility models to assess potential risk to humans from wildfires within the U.S.–Mexico Border Zone. *Prof. Geogr.* **62**, 230–247 (2010).
21. Campbell, M. J., Dennison, P. E. & Butler, B. W. A LiDAR-based analysis of the effects of slope, vegetation density, and ground surface roughness on travel rates for wildland firefighter escape route mapping. *Int. J. Wildland Fire* **26**, 884–895 (2017).
22. Richmond, P. W., Potter, A. W. & Santee, W. R. Terrain factors for predicting walking and load carriage energy costs: Review and refinement. *J. Sport Hum. Perform.* **3**, (2015).
23. Aghabayk, K., Parishad, N. & Shiawakoti, N. Investigation on the impact of walkways slope and pedestrians physical characteristics on pedestrians normal walking and jogging speeds. *Safety Sci.* **133**, 105012 (2021).

24. Meeder, M., Aebi, T. & Weidmann, U. The influence of slope on walking activity and the pedestrian modal share. *Transp. Res. Proc.* **27**, 141–147 (2017).
25. Sun, J., Walters, M., Svensson, N. & Lloyd, D. The influence of surface slope on human gait characteristics: A study of urban pedestrians walking on an inclined surface. *Ergonomics* **39**, 677–692 (1996).
26. Campbell, M. J., Dennison, P. E., Hudak, A. T., Parham, L. M. & Butler, B. W. Quantifying understory vegetation density using small-footprint airborne lidar. *Remote Sens. Environ.* **215**, 330–342 (2018).
27. Crespo-Peremach, P., Tompalski, P., Coops, N. C. & Ruiz, L. Á. Characterizing understory vegetation in Mediterranean forests using full-waveform airborne laser scanning data. *Remote Sens. Environ.* **217**, 400–413 (2018).
28. Hamraz, H., Contreras, M. A. & Zhang, J. Forest understory trees can be segmented accurately within sufficiently dense airborne laser scanning point clouds. *Sci. Rep.* **7**, 6770 (2017).
29. Wing, B. M. *et al.* Prediction of understory vegetation cover with airborne lidar in an interior ponderosa pine forest. *Remote Sens. Environ.* **124**, 730–741 (2012).
30. Markov, A., Hauser, L. & Chaabene, H. Effects of concurrent strength and endurance training on measures of physical fitness in healthy middle-aged and older adults: A systematic review with meta-analysis. *Sports Med.* **53**, 437–455 (2023).
31. Obuchi, S. P., Kawai, H., Garbalosa, J. C., Nishida, K. & Murakawa, K. Walking is regulated by environmental temperature. *Sci. Rep.* **11**, 12136 (2021).
32. Horiuchi, M., Handa, Y., Abe, D. & Fukuoka, Y. Walking economy at simulated high altitude in human healthy young male lowlanders. *Biol. Open* **5**, 1408–1414 (2016).
33. Snyder, G. I. *The 3D Elevation Program: Summary of Program Direction.* <http://pubs.er.usgs.gov/publication/fs20123089> (2012).
34. American Society for Photogrammetry and Remote Sensing (ASPRS). *LAS Specification 1.4 - R14.* [https://www.asprs.org/wp-content/uploads/2019/03/LAS\\_1\\_4\\_r14.pdf](https://www.asprs.org/wp-content/uploads/2019/03/LAS_1_4_r14.pdf) (2019).
35. Ullrich, A. & Pfennigbauer, M. Noisy lidar point clouds: Impact on information extraction in high-precision lidar surveying. In *Laser Radar Technology and Applications XXIII* vol. 10636, pp. 133–138 (SPIE, 2018).
36. R Core Team. R: A language and environment for statistical computing. R Foundation for Statistical Computing (2021).
37. Roussel, J.-R., *et al.* lidR: Airborne LiDAR data manipulation and visualization for forestry applications (2020).
38. Brubaker, K. M., Myers, W. L., Drohan, P. J., Miller, D. A. & Boyer, E. W. The use of LiDAR terrain data in characterizing surface roughness and microtopography. *Appl. Environ. Soil Sci.* **2013**, e891534 (2013).
39. Campbell, M. J., Dennison, P. E., Butler, B. W. & Page, W. G. Using crowdsourced fitness tracker data to model the relationship between slope and travel rates. *Appl. Geogr.* **106**, 93–107 (2019).
40. Dewitz, J. National Land Cover Database (NLCD) 2021 Products. U.S. Geological Survey. <https://doi.org/10.5066/P9JZ7AO3> (2023).
41. Goodchild, M. F. Beyond tobler's hiking function. *Geograph. Anal.* **52**, 558–569 (2020).
42. Herzog, I. Least-cost paths—some methodological issues. *Internet Archaeol.* **36** (2014).
43. U.S. Geological Survey. National Hydrography Dataset Plus High Resolution (NHDPlus HR) (2023).
44. Microsoft. US Building Footprints. Microsoft (2024).
45. Hijmans, R. J., Bivand, R., Pebesma, E. & Sumner, M. D. terra: Spatial data analysis (2023).
46. Etten, J. van & Sousa, K. de. gdistance: Distances and routes on geographical grids (2020).
47. Hijmans, R. J. *et al.* raster: Geographic data analysis and modeling (2022).

## Acknowledgements

We would like to thank the study subjects who contributed their time and effort to providing us with the experimental data upon which this study is based. This work was supported by the National Science Foundation (#BCS-2117865).

## Author contributions

M.J.C. and P.E.D. conceived the idea, designed the study, supervised the work, and wrote the manuscript. M.J.C., S.L.C., and P.E.D. collected the data. M.J.C. analyzed the data. All the authors read and approved the final manuscript.

## Competing interests

The authors declare no competing interests.

## Additional information

**Supplementary Information** The online version contains supplementary material available at <https://doi.org/10.1038/s41598-024-71359-6>.

**Correspondence** and requests for materials should be addressed to M.J.C.

**Reprints and permissions information** is available at [www.nature.com/reprints](http://www.nature.com/reprints).

**Publisher's note** Springer Nature remains neutral with regard to jurisdictional claims in published maps and institutional affiliations.

**Open Access** This article is licensed under a Creative Commons Attribution-NonCommercial-NoDerivatives 4.0 International License, which permits any non-commercial use, sharing, distribution and reproduction in any medium or format, as long as you give appropriate credit to the original author(s) and the source, provide a link to the Creative Commons licence, and indicate if you modified the licensed material. You do not have permission under this licence to share adapted material derived from this article or parts of it. The images or other third party material in this article are included in the article's Creative Commons licence, unless indicated otherwise in a credit line to the material. If material is not included in the article's Creative Commons licence and your intended use is not permitted by statutory regulation or exceeds the permitted use, you will need to obtain permission directly from the copyright holder. To view a copy of this licence, visit <http://creativecommons.org/licenses/by-nc-nd/4.0/>.

© The Author(s) 2024